

APPLICATIONS BULLETIN

Measurement of hardness as a function of depth in nitrided 316L stainless steel

The effects of substrate polarisation in a nitrided 316L stainless steel have been investigated [1] in an attempt to correlate processing parameters with surface mechanical properties. Nanoindentation allows the hardness to be measured at precise depths, meaning that variations in properties with nitriding depth can be evaluated. Fig. 1 shows a cross-sectional SEM micrograph of the diffusion layers of a typical nitrided stainless steel biased at -20 V. Secondary electron analysis confirmed the presence of a surface layer having a composition different to that of the saturated austenite phase (γ_N) beneath it. This MN-like CrN phase had a thickness of approximately 300 - 600 nm. The surface topography of this sample was investigated with scanning force microscopy (SFM) and the characteristic step-like grain structure is shown in Fig. 3.

Indentations were performed using the Nano Hardness Tester (NHT) at depths of 100, 200, 300, 400, 500, 750, 1000, 1250, 1500 and 1750 nm in order to evaluate the evolution of hardness with depth into the MN-like surface layer. The loading rate was kept constant and 5 indentations were made at each depth, with each measurement being made on fresh surface material. The results are summarised in Fig. 2 for four samples nitrided at different polarisation potentials and the virgin 316L substrate as a reference.

Two separate regions can be distinguished as a function of penetration depth, d_p : In the first region ($d_p < 300$ nm), the presence of a different phase (MN-like CrN) is confirmed by a sharp transition in hardness. This phase, created during the nitriding process, can be attributed to the decomposition of the γ_N phase during treatment. In the second region ($d_p > 300$ nm), the hardness gradually decreases with the -50 V sample decreasing more strongly than the others due to its lower nitrogen concentration at the surface.

[1] N. X. Randall, N. Renevier, H. Michel and P. Collignon, *Vacuum* 48 (10) (1997) 849 - 855

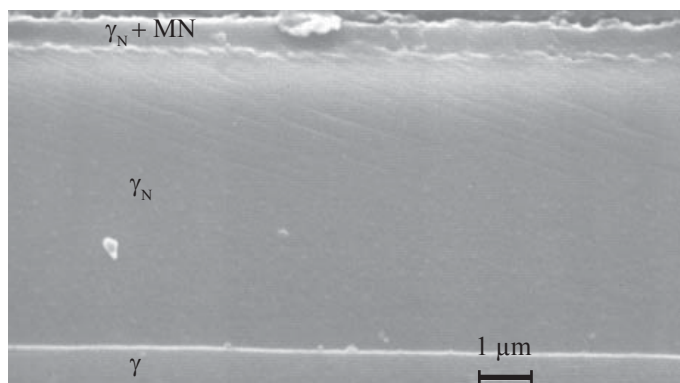


Figure 1 : Cross-sectional SEM micrograph of diffusion layers for an AISI 316L steel sample nitrided in Ar-60%N₂ during 6 h at 680 K and at 0.8 Pa on each anode at a polarisation potential of -20 V.

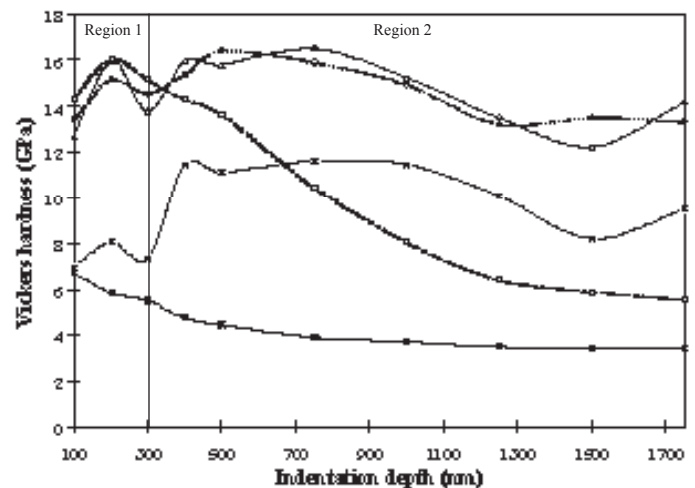


Figure 2 : Variation of nanoindentation hardness with depth below surface for the four samples nitrided at different polarisation potentials and the virgin AISI 316L substrate: (+) +20 V; (x) 0 V; (Δ) -20 V; (□) -50 V; (*) 316L substrate.

Regarding the nanoindentation profile of the 316L substrate, the hardness value stabilised to around 3.8 GPa at depths greater than about 700 nm, this correlating well with values obtained by conventional microindentation. The relatively sharp increase in hardness over the first 500 nm was attributed to a mixture of mechanical and chemical surface artefacts. The former relates to the mechanical polishing of the surface prior to nanoindentation (in this case down to a finish of 0.25 μ m using alumina paste) which is known to induce a plastically deformed layer on the surface which is significantly harder than the base material. The latter refers to the oxide and other chemical films that inevitably form on normal experimental surfaces, even if only as a result of oxidation.

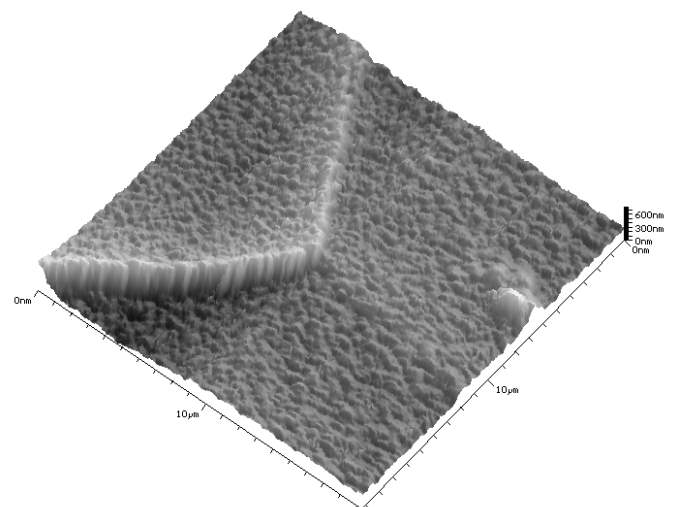


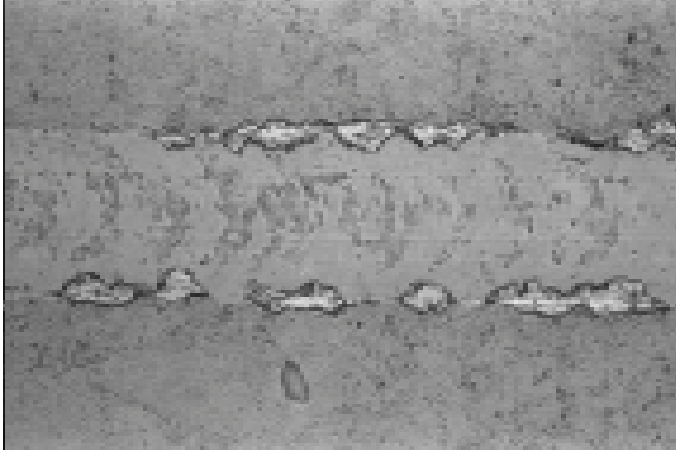
Figure 3 : Three-dimensional SFM image of nitrided surface topography (sample polarisation = -20 V) showing the step-like grain boundaries between three grains.

Scratch Test Atlas of typical failure modes obtained in scratch testing with the Revetest instrument

To enable the standardised reporting of scratch test critical load values, an atlas of scratch test failure modes has been compiled in the framework of the EC SMT project FASTE (prEN 1071-3), on the development and validation of test methods for thin hard coatings. Traceable calibration of scratch test instruments and cleaning procedures were developed in the project, and a methodology established.

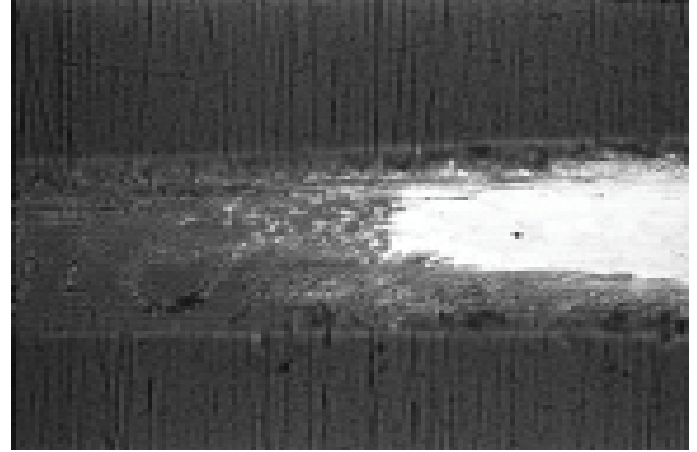
Scratches were made on a series of different coating systems. Standard scratch parameters of 100 N/min. and 10 mm/min. were used and a qualified diamond Rockwell C stylus was employed with rigorous control of the shape and cleaning prior to each test. An inventory of the major scratch test failure modes was established, which were classified into plastic deformation and different forms of cracking, spallation and coating perforation events.

Interfacial spallation at the border of the scratch track



PVD TiN (1.4 μm) on hardened and polished M2 steel (64 HRC);
 $L_c = 37 \text{ N}$

Continuous ductile perforation of the coating

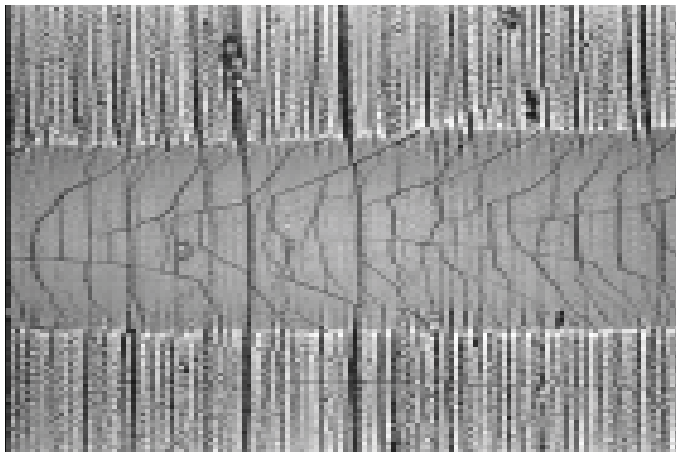


PVD DLC (3.2 μm) on hardened and ground M2 steel (64 HRC);
 $L_c = 51 \text{ N}$

Optical micrographs of a selection of failure modes are displayed on these two pages, each accompanied by a concise description of the failure mode as well as of the coating-substrate composition and the critical load value (L_c) at which the failure event occurred. All micrographs represent a magnification of 360 X. It should be noted that for each micrograph; (i) scratch direction is from left to right, (ii) the critical load values indicate when the failure event occurred initially, (iii) steel designations refer to AISI standards, (iv) hardness scales are Rockwell C Hardness (HRC, 150 kgf) and Brinell Hardness (HB, 3000 kgf, 10 mm ball).

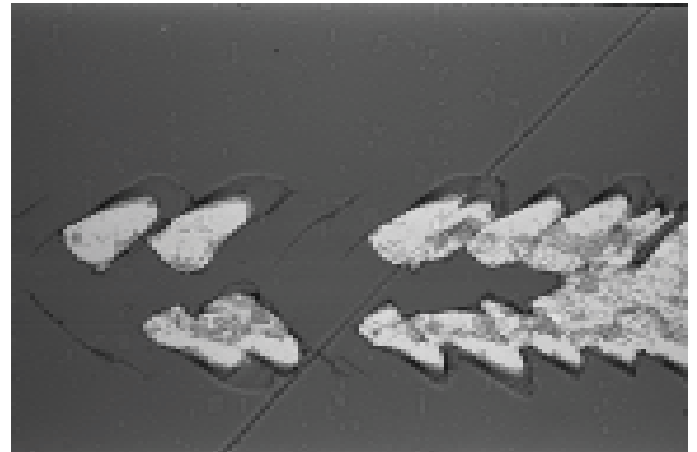
Only some of the observed failure events in scratch testing are related to detachment at the coating-substrate interface and are thus relevant as a measure of adhesion. Other failures, such as cracks and cohesive damage within the coating or substrate may be equally important to determine the behaviour of a coated component in a particular application.

Combination of chevron and hertzian cracks within the scratch track (ignore deformed grinding marks)



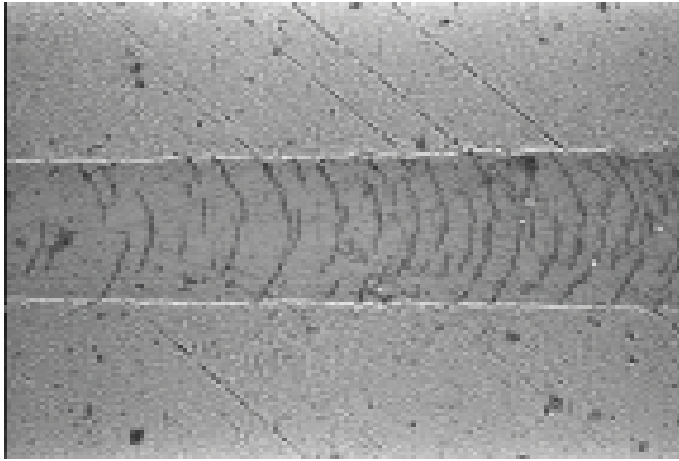
Electrolytic hard-Cr (7 μm) on hardened and ground 4137/35 steel
(56 HRC); $L_c = 5 \text{ N}$

Forward chevron cracks along scratch track with gross interfacial spallation



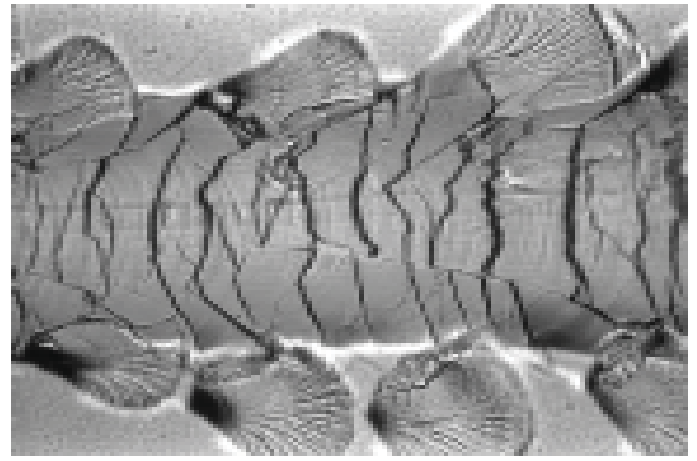
PACVD DLC (3.3 μm) on hardened and polished M2 steel (64 HRC);
 $L_c = 29 \text{ N}$

Conformal type buckling cracks



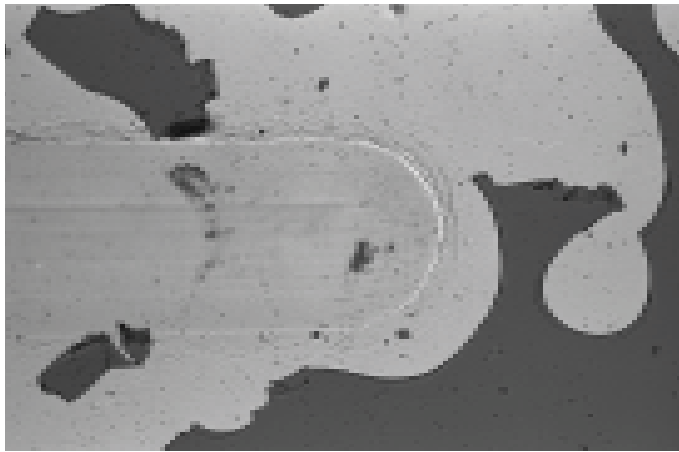
Arc-discharge DLC (0.4 μm) on annealed and polished 440B steel (260 HB); $L_c = 8\text{ N}$

Cohesive spallation along the scratch track borders



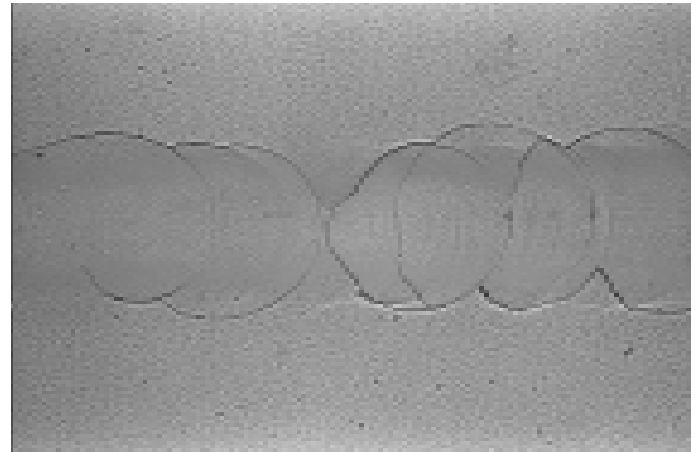
PVD AISI 316 - 10% N (10 μm) on polished 316 steel (155 HB); $L_c = 23\text{ N}$

Large area interfacial spallation



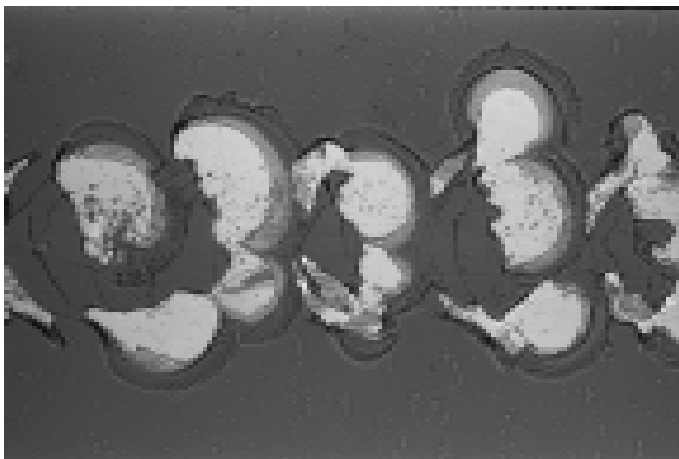
PACVD DLC (2 μm) on hardened and polished M2 steel (64 HRC); $L_c = 10\text{ N}$

Hertzian type circular cracks



PVD AISI 316 - 10% N (10 μm) on polished 316 steel (155 HB); $L_c = 28\text{ N}$

Gross interfacial shell-shaped spallation along the scratch track



PACVD DLC (3.3 μm) on hardened and polished M2 steel (64 HRC); $L_c = 43\text{ N}$

The present catalogue of scratch test failure modes cannot claim to be comprehensive, although it should be regarded as an important step towards standardised reporting of scratch test critical loads.

It should be remembered, however, that for assessing the quality of a coated component, the magnitude of and subtle differences in the observed failure event may often be equally important as the failure mode itself. In addition, there is still much research work to be carried out in order to understand more fully the mechanisms of each failure mode. The results of this study will be used for producing an improved European Standard on the scratch test, based on earlier work within the European Standards working group CEN TC 184/WG 5 "Test Methods for Ceramic Coatings".

The complete scratch test atlas can be purchased in poster format from CSEM Instruments for a fee of \$150.

High-Temp. Tribometer for friction comparison of automobile brake pad materials

The most important property of brake pads in automobile applications is the friction coefficient between the static pad and the rotating disk against which it makes contact. Parameters of secondary importance include the wear rate of the pad material and the influence of service temperature fluctuations on the frictional properties.

This study was carried out in order to compare the frictional properties of three different brake pad materials, two of which contain an asbestos addition called chrysotile which is still commonly used for high-friction applications. Testing was performed using a CSEM High Temperature Tribometer (HTT) using a static partner of 100Cr6 steel, an applied load of 5 N, a sliding speed of 10 cm s⁻¹, a wear radius of 10 mm and a total distance corresponding to 10 000 rotations. Different measuring temperatures in the range 23 - 200 °C were used.

The optical micrographs in Fig. 1 show the differences in the observed wear track between two samples, one with and one without asbestos addition. For all measurement temperatures it was found that the asbestos samples had a smoother wear track and less wear than the non-asbestos sample.

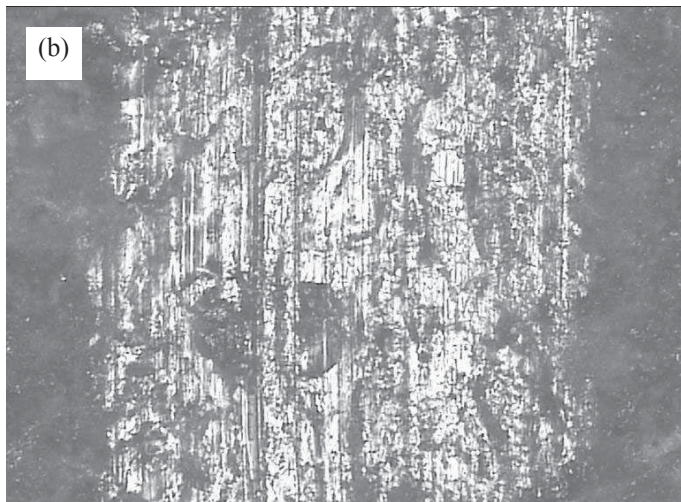
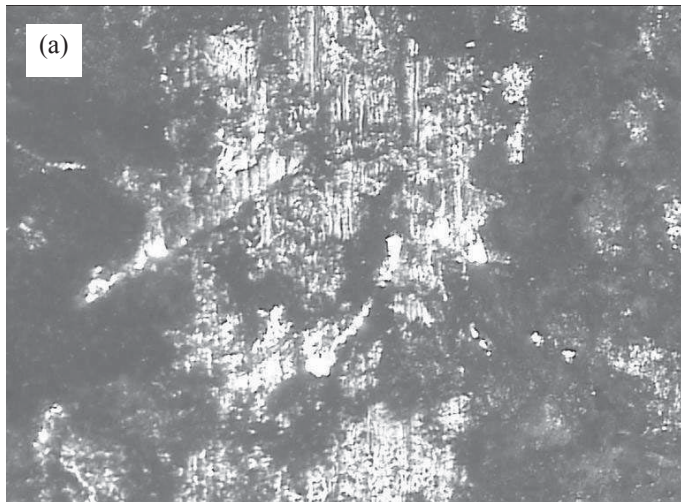


Figure 1 : Optical micrographs (50X) of wear tracks on (a) a non-asbestos sample and (b) an asbestos sample after high-temperature testing at 50°C over 10 000 laps with an applied load of 5 N and speed 10 cm s⁻¹.

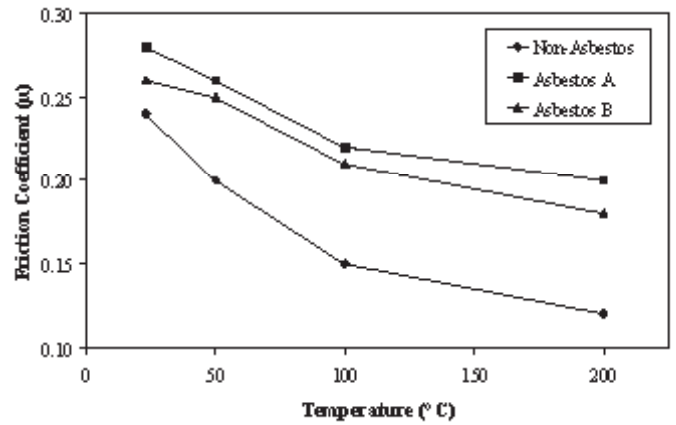


Figure 2 : Friction coefficients plotted as a function of measurement temperature for the non-asbestos and the two asbestos samples. Note that the reduction in friction as temperature increases is less steep for the samples containing asbestos.

However, the friction results summarised in Fig. 2 show that both asbestos samples maintained higher friction coefficients at elevated temperatures than the non-asbestos sample. This is particularly interesting as brake pads can get quite hot during normal service and tend to lose their efficiency at elevated temperatures (also known as *brake fade*).

These results suggest that asbestos can be a very useful addition to any material which must provide a high friction coefficient but a low rate of wear. Currently, the use of asbestos in such applications is diminishing due to the health risks involved as a result of inhalation of asbestos particles. Various alternative materials are now available but seem to still be considerably more expensive. The High Temperature Tribometer is ideally suited to this kind of testing where in-service conditions can be accurately simulated.

CSM
+
Instruments

This Applications Bulletin is published quarterly and features interesting studies, new developments and other applications for our full range of mechanical surface testing instruments.

Editor

Dr. Nicholas Randall

Should you require further information, then please contact:

CSM Instruments
Rue de la Gare 4
CH-2034 Peseux
Switzerland

Tel: + 41 32 557 5600
Fax: +41 32 557 5610
info@esm-instruments.com
www.esm-instruments.com

DISTRIBUTOR: